DOI: 10.26599/FSHW.2026.9251188

Contents lists available at SciOpen

Food Science and Human Wellness

journal homepage: https://www.sciopen.com/journal/2097-0765

China Food Publishing Co.

Deciphering the mechanisms of *Limosilactobacillus fermentum* A51 involved in exopolysaccharides biosynthesis regulated by LuxS/AI-2-QS system

Guangqiang Wei[a#], Daodian Wang[ab#], Teng Wang[a], Yunmei Chai[a], Wentao Zheng[a], Yuzhu Wang[a], Wenbin Zhang[a], Aixiang Huang[a]*, Yufang Li[a]

[a]*College of Food Science and Technology, Yunnan Agricultural University, Kunming 650201, Yunnan, China*

[b]*Sericulture and Apiculture Research Institute, Yunnan Academy of Agricultural Sciences, Mengzi, 661101, China*

ABSTRACT: *Limosilactobacillus fermentum* A51 is a high Exopolysaccharides (EPS) producing strain harboring the S-ribosylhomocysteinase/autoinducer-2-quorum sensing (LuxS/AI-2-QS) system. However, the regulatory mechanism of EPS synthesis by this system remains unclear. In this study, we combined biochemical, proteomic, and parallel reaction monitoring (PRM) analyses to elucidate the role of the LuxS/AI-2-QS system in EPS biosynthesis. Biochemical results indicated that 200 μmol/L furanone inhibitor could downregulate *luxS* and *eps* gene expression, reducing the AI-2 activity and EPS yield (decreased from 459.87 mg/L to 439.26 mg/L) and monosaccharide yield ($P < 0.05$), thereby blocking the LuxS/AI-2-QS system and EPS biosynthesis of *L. fermentum* A51. Thus, the LuxS/AI-2-QS system positively regulates EPS synthesis. Furthermore, tandem mass tags (TMT)-based quantitative proteomics identified 512 differentially expressed proteins (DEPs) between normal and furanone-inhibited groups. Among them, 32 downregulated DEPs in the inhibited-group, and they were involved in the LuxS/AI-2-QS system and Wzx/Wzy-dependent pathway. PRM validation confirmed twelve key proteins, including AI-2 synthesis protein LuxS, AI-2 export transporter (AI-2E), and the EPS biosynthesis-related proteins glycosyl transferase, glucokinase, flippase (Wzx), and polymerase (Wzy). Overall, this study provides novel insights into the LuxS/AI-2-QS system regulating EPS biosynthesis of LAB by mediating the Wzx/Wzy pathway, which might promote development of new approaches for EPS biosynthesis based on QS target.

Keywords: *Limosilactobacillus fermentum* A51; exopolysaccharides; autoinducer-2; wzx/wzy pathway; quantitative proteomics

1. Introduction

Bacteria carry out inter- and intra-species communications through the quorum sensing (QS) system. Several studies have reported that lactic acid bacteria (LAB) communicate via the signalling molecule autoinducer-2 (AI-2) [1-3]. The LuxS/AI-2-QS system is a population density-dependent regulatory mechanism [4]. LAB exchange information through the production, release, accumulation, and sensing of the AI-2 signal molecule, ultimately enabling multiple lactobacilli to cooperate in performing specific physiological functions. Recent studies indicate that the synthesis of probiotic factors in *Lactiplantibacillus*

[#]Contributed equally to this work.
***Corresponding author**
aixianghuang@126.com (Aixiang Huang).

Received 9 October 2025
Received in revised from 16 December 2025
Accepted 11 February 2026

plantarum and *Limosilactobacillus fermentum* is closely linked to the regulation of the LuxS/AI-2-QS system. These factors include biofilm formation, production of phenyllactic acid, production of conjugated linoleic acid, production of gamma-aminobutyric acid, and bacteriocin synthesis [2,5-8]. For instance, quorum sensing inhibitors (QSIs) inhibit the LuxS/AI-2 pathway, downregulating *luxS* expression and disrupting central metabolic pathways, which ultimately impairs biofilm development in *L. fermentum* [9]. Similarly, QSIs can block this signaling system and reduce conjugated linoleic acid production [6]. Together, these findings highlight the LuxS/AI-2 system as a central regulator of probiotic metabolite biosynthesis in LAB.

LAB exopolysaccharide (EPS) is a secondary metabolite secreted outside the cell wall during the growth and metabolism of LAB. EPS produced by LAB possesses unique physicochemical properties and is widely used in the "clean label" food industry to improve viscosity, mouthfeel, and textural properties [10]. Additionally, EPS has various biological activities, including antioxidant, antibiofilm, antitumor, anti-inflammatory, hypoglycemic, and cholesterol-lowering effects, making it a valuable component in probiotic development [11]. Therefore, EPS has become a research hotspot in the study of functional components of LAB in recent years. Current research on EPS biosynthesis mainly focuses on known high-yielding EPS strains. However, in-depth studies on the regulatory mechanism of the LuxS/AI-2-QS system on EPS biosynthesis of LAB are still lacking. Recent studies have reported a coordinated relationship between the secretion of AI-2 and EPS biosynthesis in LAB. Ji [12] revealed a positive relationship between the AI-2 activity and EPS production in *Lactiplantibacillus plantarum* 5-4-1 and *Pediococcus acidilactici* TG1-1-10. Further studies demonstrated that the addition of 60 μmo1/L exogenous AI-2 resulted in a four-fold increase in EPS yield by *L. plantarum* 5-4-1 [13]. Wang et al. [14] also found that the addition of 100 μmol/L of exogenous AI-2 promoted EPS production in *L. fermentum* TG4-1-1 and *Pediococcus acidilactici* 11-3. Additionally, an in-depth study revealed that knocking out the *luxS* gene, which regulates AI-2 biosynthesis in *L. fermentum*, reduces the EPS yield [15]. Although studies have demonstrated a positive relationship between the LuxS/AI-2-QS system and EPS biosynthesis, the underlying regulatory mechanisms remain poorly understood. Given the broad influence of LuxS/AI-2-QS system on diverse probiotic traits, it is compelling to explore its role in the synthesis of EPS in LAB.

The biosynthesis of LAB derived EPS typically involves four main pathways: the extracellular biosynthesis pathway, the synthase-dependent pathway, the ATP-binding cassette (ABC) transporter-dependent pathway, and the Wzx/Wzy-dependent pathway [11]. Among them, the Wzx/Wzy-dependent pathway is most common in LAB [16]. The Wzx/Wzy pathway consists of five main steps: monosaccharide phosphorylation or transportation, biosynthesis of nucleotide sugar, biosynthesis of repeating units, transfer position of repeating units, and polymerization and export of long chains. Regulatory proteins play a direct role in modulating the Wzx/Wzy-dependent pathway in LAB [17,18]. In recent years, proteomic approaches have been extensively applied to identify critical regulatory proteins in LAB [7,19]. For instance, Ma et al. [6] demonstrated through proteomics analysis that the S-Ribosylhomocysteinase (LuxS) protein regulates conjugated linoleic acid production by modulating

enolase (eno) expression. Similarly, Chai et al. [7] demonstrated that the LuxS protein regulated the production of phenyllactic acid by modulating aminotransferase (araT) and lactate dehydrogenase (ldh) expression. However, the lack of specific antibodies for immunoblot analysis complicates the validation of regulatory proteins identified through proteomics. Parallel Reaction Monitoring (PRM) is an antibody-free, absolute quantitative technology based on targeted mass spectrometry [20,21]. This method has significant advantages in the quantitative analysis of proteins due to its high sensitivity and specificity and ability to cover a high dynamic range [22,23]. Therefore, combining proteomics and PRM presents a promising potential for comprehensively unraveling and validating the regulatory mechanisms of the LuxS/AI-2-QS system on EPS biosynthesis of LAB.

In our previous study, a high EPS-producing *L. fermentum* A51 was isolated from naturally fermented yak yogurt and successfully applied in yogurt processing [24]. Additionally, the EPS yield positively correlated with the activity of the signaling molecule AI-2 [25]. However, the regulatory relationship between the LuxS/AI-2-QS system and EPS biosynthesis and its regulatory mechanism remains unclear. Thus, AI-2 activity, EPS yield, and *luxS* and *eps* genes expression were determined before and after QSIs treatment to clarify the regulatory relationship between LuxS/AI-2-QS system and EPS biosynthesis. Then, key regulatory proteins involved in LuxS/AI-2-QS system-mediated EPS biosynthesis were identified and validated using proteomics and PRM technology. Furthermore, the underlying mechanism of the LuxS/AI-2-QS system regulating EPS biosynthesis through the Wzx/Wzy pathway was analysed. This study provides novel insights into the regulatory role of the LuxS/AI-2-QS system in EPS biosynthesis and its significance in EPS production by LAB.

2. Materials and methods

2.1. Bacterial strain and materials

The EPS-producing strain *L. fermentum* A51 (GenBank accession no. PRJNA1001634), used in this study, was isolated from traditional fermented yak yogurt collected in Yunnan Province, China. Strain identification was performed through Gram staining, morphological characterization, and 16S rDNA sequencing. The strain has been deposited in the China Center for Type Culture Collection (CCTCC; accession no. M 2023861) and is maintained at −80 °C in 20% (v/v) glycerol-supplemented nutrient broth at the College of Food Science and Technology, Yunnan Agricultural University (Kunming, China). For the LuxS/AI-2-QS system assays, *Vibrio harveyi* BB170 (ATCC BAA-1117), employed as the reporter strain, was obtained from the Guangdong Microbial Culture Collection Center (GDMCC).

The de Man, Rogosa, and Sharpe (MRS) broth was purchased from Beijing Solarbio Science & Technology Co., Ltd. Beijing, China. Furanone was (analytical grade) purchased from Shanghai Aladdin Biochemical Technology Co., Ltd. Shanghai. Anhydrous acetonitrile, dithiothreitol, hydroxylamine (analytical grade), were purchased from Sigma-Aldrich (3050 Spruce Street, St. Louis, USA). RNA Extraction Kit and Goldenstar RT6 cDNA Synthesis Kit Ver 2 were purchased from Beijing Tsingke Biotech Co., Ltd. Beijing.

2.2. Determination of the effect of different concentrations of QSIs on EPS production by L. fermentum A51

Sterilized MRS liquid medium was supplemented with QSIs (furanone) filtered through a 0.22 μm water-based membrane to achieve final furanone concentrations of 0, 50, 100, 150, 200, 250, and 300 μmol/L. After the activation of *L. fermentum* A51, the strain was inoculated into the QSIs-supplemented MRS liquid medium and and incubated statically at 37 °C for 18 hours. The fermentation broth was centrifuged at 6,250 rcf for 15 min at 4 °C to obtain cell-free supernatant (CFS). Then, trichloroacetic acid (TCA) at a final concentration of 4% was added to the CFS to remove proteins. The solution was centrifuged at 8,000 rcf for 15 min at 4 °C to obtain supernatant. The supernatant was concentrated to one-third of its original volume; and after chilled ethanol at three times its volume was added, it was stored overnight at 4 °C. The precipitate was collected and redissolved in deionized water. After dialysis and lyophilization, EPS produced by *L. fermentum* A51 was obtained, and the EPS content was determined by phenol-sulfuric acid method.

2.3. Determination of the effect of QSIs on EPS biosynthesis of L. fermentum A51

L. fermentum A51, at a cell concentration of 1.5×10^9 CFU/mL, was inoculated in two conditions: 3% (v/v) into MRS medium (normal-group) and MRS medium containing 200 μmol/L furanone as a QSIs (inhibited-group). Cultures were incubated at 37 ℃ for 24 h. Subsequently, bacterial growth, colony morphology, activity of AI-2 signaling molecule, EPS yield, monosaccharide composition of EPS, and *eps* gene expression levels of *L. fermentum* A51 were determined.

2.3.1. Determination of the effect of QSIs on the growth of L. fermentum A51

The absorbance values of the fermentation broth at OD_{600} nm were recorded at 2-h intervals over the 24-h incubation period of *L. fermentum* A51 in both the normal- and inhibited-group. A growth curve was subsequently constructed, with time represented on the horizontal axis and absorbance values on the vertical axis.

2.3.2. Determination of the effect of QSIs on the AI-2 activity of L. fermentum A51

The effect of QSIs on the AI-2 activity of *L. fermentum* A51 was determined according to the method of Ma et al. [6]. *Vibrio harveyi* (*V. harveyi*) BB170 was cultured overnight in AB medium until the OD_{600} nm reached 0.9-1.1. The *V. harveyi* BB170 solution was diluted with fresh AB medium at a volume ratio of 1:100. Sterile supernatants (obtained by filtering through a 0.22 μm microbial filter) for *L. fermentum* A51 in the normal- and inhibited-groups incubated at 37 °C for 0, 4, 8, 12, 16, 20 and 24 h, negative control and medium control were mixed with the diluted *V. harveyi* BB170 solution at a volume ratio of 1:50 and incubated at 100 rpm and 30 ℃ in a shaker (Shanghai Zhichu Instrument Co., Ltd. Shanghai, China). When the negative control had the lowest fluorescence intensity, the fluorescence intensity of each sample was measured at 490 nm using an enzyme-labeled reader (Multiskan FC, Thermo Fisher Scientific), and its relative fluorescence intensity, which represents the AI-2 activity, was calculated.

$$\text{Relative fluorescence intensity of the sample} = \frac{\text{Fluorescence intensity value of the sample}}{\text{Fluorescence intensity value of the medium control}}$$

2.3.3. Determination of the effect of QSIs on the EPS yield of L. fermentum A51

L. fermentum A51 was inoculated at 5% (v/v) in fresh MRS medium and MRS medium containing QSIs and incubated at 37 °C for 0, 4, 8, 12, 16, 20 and 24 h. Then, determine the EPS yield of *L. fermentum* A51 at different fermentation times using the method described in Section 2.2.

2.3.4. Determination of the effect of QSIs on the colony morphology of L. fermentum A51

One milliliter of third-generation *L. fermentum* A51 was serially diluted to 10^{-6}, and spread on MRS solid medium and MRS solid medium containing QSIs. The medium was then incubated at 37 ℃ for 24 h. Then, the morphology of *L. fermentum* A51 was observed using biological scanning electron microscopy (SEM). Briefly, cells were obtained by centrifugation at 8,000 rcf, 4 ℃ for 10 min, then washed twice with phosphate buffer (0.1 M, pH 7.2). The cells were fixed with 2.5% glutaraldehyde for 12 h and washed three times with phosphate buffer. Next, gradient dehydration with ethanol was performed for 10 min each time, and bacteria were precipitated by centrifugation at 8,000 rcf, 4 ℃ for 10 min. Tert-butanol was used instead of ethanol for centrifugation. The bacteria were diluted with phosphate buffer, dropwise freeze-dried on slides, and sputter-coated with gold [26]. Finally, cells were observed using a regulus 8100 biological SEM (Hitachi Ltd., Tokyo, Japan).

2.4. Effect of QSIs on the monosaccharide composition of EPS

The effect of QSIs on the monosaccharide composition of *L. fermentum* A51 EPS was determined following the method described by Wang et al. [27]. An ion chromatography system (ICS-5000, Thermo Fisher Scientific, USA), equipped with a Dionex™ CarboPac™ PA20 column (150 × 3.0 mm, 10 μm), was used to analyze the monosaccharide composition. The injection volume was 5 μL, and the column temperature was 30 ℃. The mobile phases A, B and C were water, 0.1 M sodium hydroxide, and 0.1 M NaOH containing 0.2 M CH_3COONa, respectively. Quantification was performed using an external standard method.

2.5. Quantitative real-time PCR analysis the expression levels of eps genes

Total RNA was isolated from *L. fermentum* A51 of normal- and inhibited-groups using RNA Extraction Kit (Beijing Tsingke Biotech Co., Ltd., Beijing, China). The A260/280 ratios of the extracted RNA were about 2.1. The total RNA was reverse-transcribed into cDNA using Goldenstar RT6 cDNA Synthesis Kit Ver 2. Real-time PCR analysis of candidate genes, including *luxS*, UDP-galactopyranose mutase (*glf*), Glycosyl transferase (*gtf*), chain-length regulatory proteins (*Wzz*), polymerase (*Wzy*), and flippase (*Wzx*) were performed using ABI, QuantStudioTM 1 Plus real-time fluorescence quantitative PCR instrument (Thermo Fisher, USA). Gene-specific primers used in the experiment are listed in Table 1. *lfe* gene was used as an internal reference gene. The *eps* genes were analyzed using the $2^{-\Delta\Delta Ct}$ method. In addition, QSIs were added to *L. fermentum* A51 fermentation broth to investigate the effect of QSIs on the expression level of *eps* genes in *L. fermentum* A51. All experiments included three independent biological replicates.

Table 1 Sequences of primers used for real-time quantitative PCR.

Name	Sequence (5′–3′)
Lfe-16S-F	TGGGCGTAAAGAGAGTGCAG
Lfe-16S-R	TCTACGCATTCCACCGCTAC
luxS-F	AGAAATCGCCTACCACACCG
luxS-R	GACCATTCCTTGGCGGAGAA
glf-F	CCAAGAAATGGCCGGCAAGA
glf-R	TGGCAGGCGACGAATAATGA
gtf-F	CGTCGATGATGGATCAACTGATAA
gtf-R	GGCAGCACTAACTCCACCAT
Wzz-F	ACGGTAAGCACCCAAACCAA
Wzz-R	TCTTGTTCGGGAAGGACTGG
Wzx-F	TGTTGTTGATGCCGCAAAGA
Wzx-R	GATTAACCCAACTGCCACCC
Wzy-F	AGTAACGAATGAGCGTCAAGAGA
Wzy-R	CATCGCACCTGTCTTGCCTA

2.6. Tandem mass tags (TMT)-quantitative proteomics analysis

2.6.1. Protein extraction

Protein was extracted following the method described by Ma et al. [28] with slight modifications. *L. fermentum* A51 was cultured in MRS broth, while the inhibited-group were cultured in MRS liquid medium containing QSIs. The supernatant was removed by centrifugation (8,000 rcf, 4 ℃, 15 min), and the precipitate was washed three times with PBS. A 350 μL Radioimmunoprecipitation assay buffer was added to 200 μL bacterial samples and sonicated for 10 min at 4 ℃. The resulting supernatant was collected by centrifugation at 10,000 rcf and 4 ℃ for 15 min. Protein concentration in the supernatant was quantified using the bicinchoninic acid (BCA) protein quantification kit (Beyotime, Shanghai, China). A 100 μg protein sample was diluted to 1 mg/mL, and five volumes of pre-cooled acetone were added for precipitation overnight -20 ℃. The precipitate was collected by centrifugation at 10,000 rcf and 4 °C for 10 min, washed twice with 200 μL of pre-cooled 80% acetone, and centrifuged again to remove the supernatant. Subsequently, the precipitate was treated with 5 mM dithiothreitol and incubated at 55 ℃ for 20 min to reduce the disulfide bonds. After cooling to room temperature, 15 mM of iodoacetamide was added and allowed to react for 30 min in the dark. All experiments included three independent biological replicates.

2.6.2. Protein digestion and TMT labeling

Trypsin was dissolved in resuspension buffer to a concentration of 0.5 μg/μL and incubated for 5 min at room temperature. The trypsin solution was then combined with the sample protein at a 1:50 trypsin-to-protein ratio and incubated overnight at 37 ℃ with shaking at 800 rpm. After incubation, the protein precipitate was collected by centrifugation at 10,000 rcf for 15 min at 4 ℃. The resulting protein was transferred to a new eppendorf tube and labeled according to the manufacturer's instructions (TMT Isobaric Label Reagent Set, Thermo Scientific, Rockford, USA). Subsequently, the labeled samples underwent sodium deoxycholate cleanup, peptide desalting, and high-pH pre-fractionation in preparation for Nano LC-MS/MS analysis.

2.6.3. Nano LC-MS/MS analysis

LC-MS/MS analysis was performed following the procedure described by Chai et al. [8]. Each sample containing 2 μg of total peptides was separated and analyzed with a Nano UPLC (EASYnLC1200) coupled to a Q Exactive HFX Orbitrap instrument (Thermo Fisher Scientific, Rockford, USA) equipped with a nano-electrospray ion source. A reversed-phase column (100 μm ID × 15 cm, Reprosil-Pur 120 C18-AQ, 1.9 μm, Dr. Maisch) was used for separation. The mobile phases comprised H_2O with 0.1% FA and 2% ACN as mobile phase A and 80% ACN with 0.1% FA as mobile phase B. Gradient elution was performed over 90 min at a flow rate of 300 nL/min, with the gradient profile as follows: 2-5% B for 2 min, 5-22% B for 68 min, 22-45% B for 16 min, 45-95% B for 2 min, and 95% B for 2 min. Data dependent acquisition (DDA) was performed in profile and positive mode using Orbitrap analyzer, with MS1 scans conducted at a resolution of 120,000 (at 200 m/z) and an m/z range of 3501600. For MS2 scans, a resolution of 45,000 was used, with a fixed first mass of 110 m/z. The automatic gain control target was set to 3E6 with a maximum injection time of 30 ms for MS1 and 1E5 with a max IT of 96 ms for MS2. Fragmentation of the top 20 most intense ions was performed by HCD with a normalized collision energy of 32% and an isolation window of 0.7 m/z. Dynamic exclusion was set to 45 s, ions with single charged peaks or charges exceeding 6 were excluded from the DDA procedure.

2.6.4. Database search and quantification

Vendor-provided raw MS files were processed using Proteome Discoverer (PD) software (Version 2.4.0.305) and the built-in Sequest HT search engine. The MS spectra lists were searched against species-level UniProt FASTA databases for *Limosilactobacillus fermentum* (Proteome ID: UP0001613, release date: 2022-12-28), with Carbamidomethyl [C] set as a fixed modification for TMT 6 plex (K) and TMT 6 plex (N-term), and Oxidation (M) and Acetyl (Protein N-term) as variable modifications. Trypsin was used as the protease, with a maximum of 2 missed cleavages allowed. The false discovery rate (FDR) was set to 0.01 for both PSM and peptide levels. Peptide identification utilized an initial precursor mass deviation of up to 10 ppm and a fragment mass deviation of 0.02 Da. Unique and razor peptides were used for protein quantification, while total peptide amount was used for normalization. All other parameters were kept as default settings.

2.6.5. Bioinformatics analysis

The databases of Gene Ontology (GO, http://www.geneontology.org/), COG (Clusters of Orthologous Groups) and Kyoto Encyclopedia of Genes and Genomes (KEGG, https://www.genome.jp/kegg/) were used to analyze the protein family and pathway. Differentially expressed proteins were used for volcanic map analysis, cluster heat map analysis and enrichment analysis of GO and KEGG.

2.7. PRM verified key proteins

PRM analysis was conducted to validate the DEPs obtained through proteomic analysis. All experiments included three independent biological replicates. *L. fermentum* A51 samples were prepared using the same procedure as in the proteomics analysis. After protein extraction and trypsin digestion, the

mixture was loaded directly onto a reversed-phase column (PePSep C18, 1.9 μm, 75 μm × 15 cm, Bruker, Germany). Peptides were analyzed using a tims TOF Pro2 instrument (Bruker) with a nano-electrospray ion source. Vendor-provided raw MS files were processed using SpectroDive (11.10.230428.47784), the Pulsar search engine, and other established libraries. A panel of screening peptides and secondary b/y ions were quantified. A maximum of 2 specific peptides were selected for each protein, with 3-6 fragment ions chosen for quantification per target peptide. The identified peptide spectrum matches and protein were retained and performed with FDR no more than 0.01.

2.8. Data analysis

Experimental data were presented as mean ± SD of triplicate measurements. Descriptive data and the differences between samples were analyzed by ANOVA and Duncan's test using SPSS (SPSS Inc., Chicago, IL, USA). $P < 0.05$ was considered as significant difference. All the figures were generated using the Origin Pro software (Origin-Lab, version 2021, USA).

3. Results

3.1. LuxS/AI-2-QS system-mediated EPS biosynthesis of L. fermentum A51

3.1.1. Effect of QSIs on EPS biosynthesis of L. fermentum A51

Furanones have a structural similarity to the signaling molecule AI-2 and inhibit the QS systems of LAB by competitively binding to the corresponding AI-2 receptors. Because of this mechanism, furanones are important QSIs for suppressing the LuxS/AI-2-QS system in various strains of *L. fermentum*, including *L. fermentum* B41, *L. fermentum* L1, and *L. fermentum* A119 [5,29]. This study determined the effect of different concentrations of furanone on the EPS production and signaling molecule AI-2 activity of *L. fermentum* A51. As shown in Fig. 1A, compared with the normal group (0 μmol/L), furanone concentrations ranging from 100 to 250 μmol/L significantly inhibited EPS production in *L. fermentum* A51 ($P < 0.05$). Furthermore, as the concentration of furanone increased, its inhibitory effect on the AI-2 activity of *L. fermentum* A51 gradually intensified, with the most pronounced inhibition observed at 200 μmol/L. However, when the concentration of furanone was raised to 250 μmol/L, the AI-2 activity increased. This may be due to the structural similarity of furanone compounds to AI-2 signaling molecules. At certain concentrations, they can suppress AI-2 activity, whereas beyond this threshold, furanone compounds may instead promote the strain's capacity to produce AI-2. Therefore, 200 μmol/L was selected as the optimal inhibitory concentration. However, the current study only measured the activity of extracellular AI-2, whereas future research incorporating measurements of intracellular AI-2 activity could provide deeper insights into the underlying regulatory mechanisms.

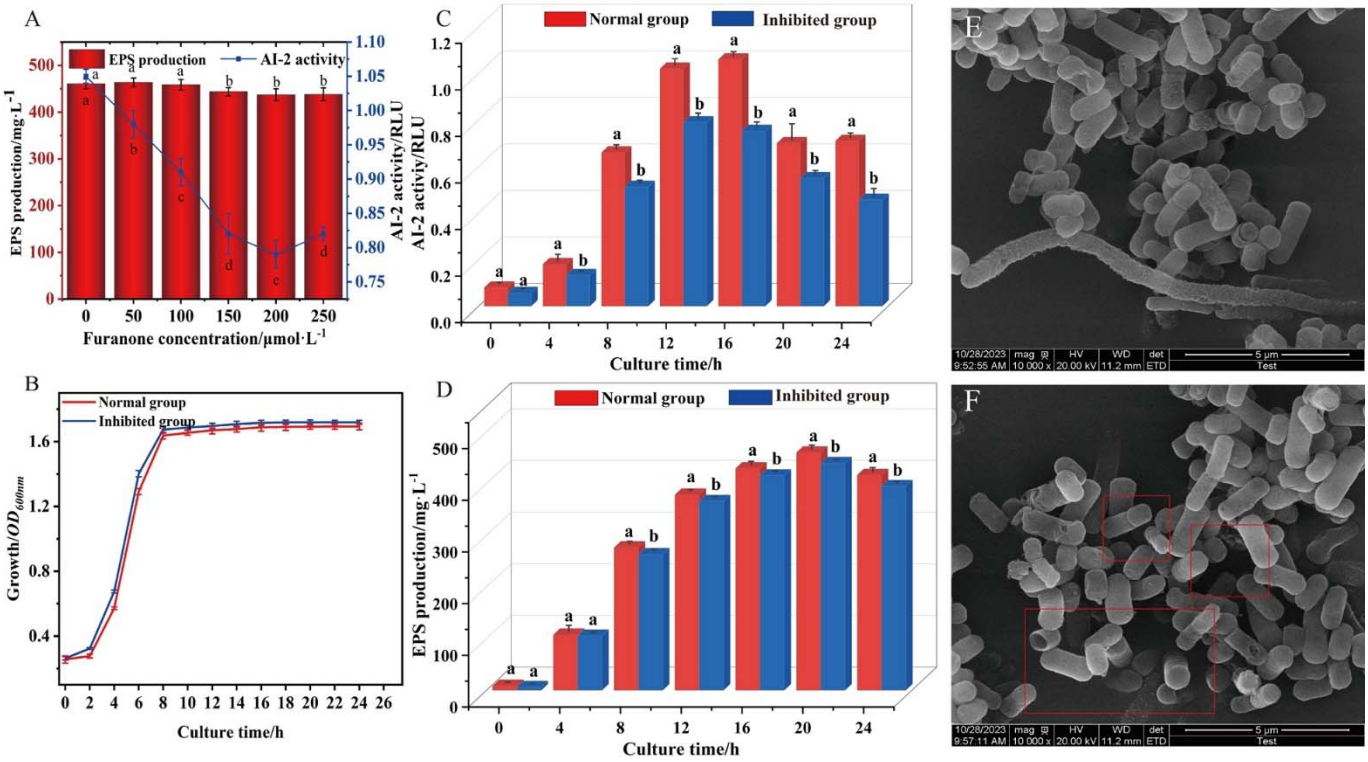

Figure 1. Effects of adding furanone on *L. fermentum* A51. (A) EPS yield and AI-2 activity. (B) Growth. (C) AI-2 activity. (D) EPS yield. (E) Morphology of normal group. (F) Morphology of inhibited group. AI-2: Autoinducer-2; EPS: exopolysaccharides. Different superscripted lowercase letters indicate $P < 0.05$.

The effect of QSIs (furanone, 200 μmol/L) on the growth of *L. fermentum* A51 over a during 24 h incubation period was assessed. The results demonstrated that both the normal- and inhibited-groups reached the lag, logarithmic, stationary, and death phases at comparable time points, indicating that QSIs did not affect the growth pattern of *L. fermentum* A51 (Fig. 1B). The influence of QSIs on the activity of the AI-2 signaling molecule in *L. fermentum* A51 was evaluated. The results showed that during incubation, the AI-2 activity in the inhibited-group was significantly lower than that in the normal-group ($P < 0.05$), indicating that QSIs effectively inhibited the LuxS/AI-2-QS system of *L. fermentum* A51 (Fig. 1C). Additionally, the effect of QSIs on EPS yield in *L. fermentum* A51 was investigated. At the early stage of the inhibited-group (0 to 4 h), QSIs did not affect EPS production, likely due to the inactivation of the LuxS/AI-2-QS system during this period [5]. As depicted in Fig. 1D, at 20 h, the maximum EPS yield was significantly reduced from 459.87 ± 8.43 mg/L to 439.26 ± 2.18 mg/L ($P < 0.05$). This inhibition occurred because QSIs competitively inhibited the LuxS/AI-2-QS system by competing with the receptor alongside the signaling molecule AI-2, thus influencing the expression of *eps* genes and decreasing EPS yield.

The effects of QSIs on the morphology of *L. fermentum* A51 were observed using a regulus biological SEM. As illustrated in Fig. 1E under normal conditions, *L. fermentum* A51 exhibited a long, rod-shaped morphology, adhering in clusters with rounded and intact hyphae. In contrast, after the addition of QSIs, while the overall morphology and surface smoothness of the organisms remained unchanged, they appeared more scattered and loosely distributed, and the adhesion and aggregation between bacteria were reduced

(Fig. 1F). Further observation under an optical microscope revealed that QSIs inhibited the adhesion of *L. fermentum* A51 (Fig. 2).

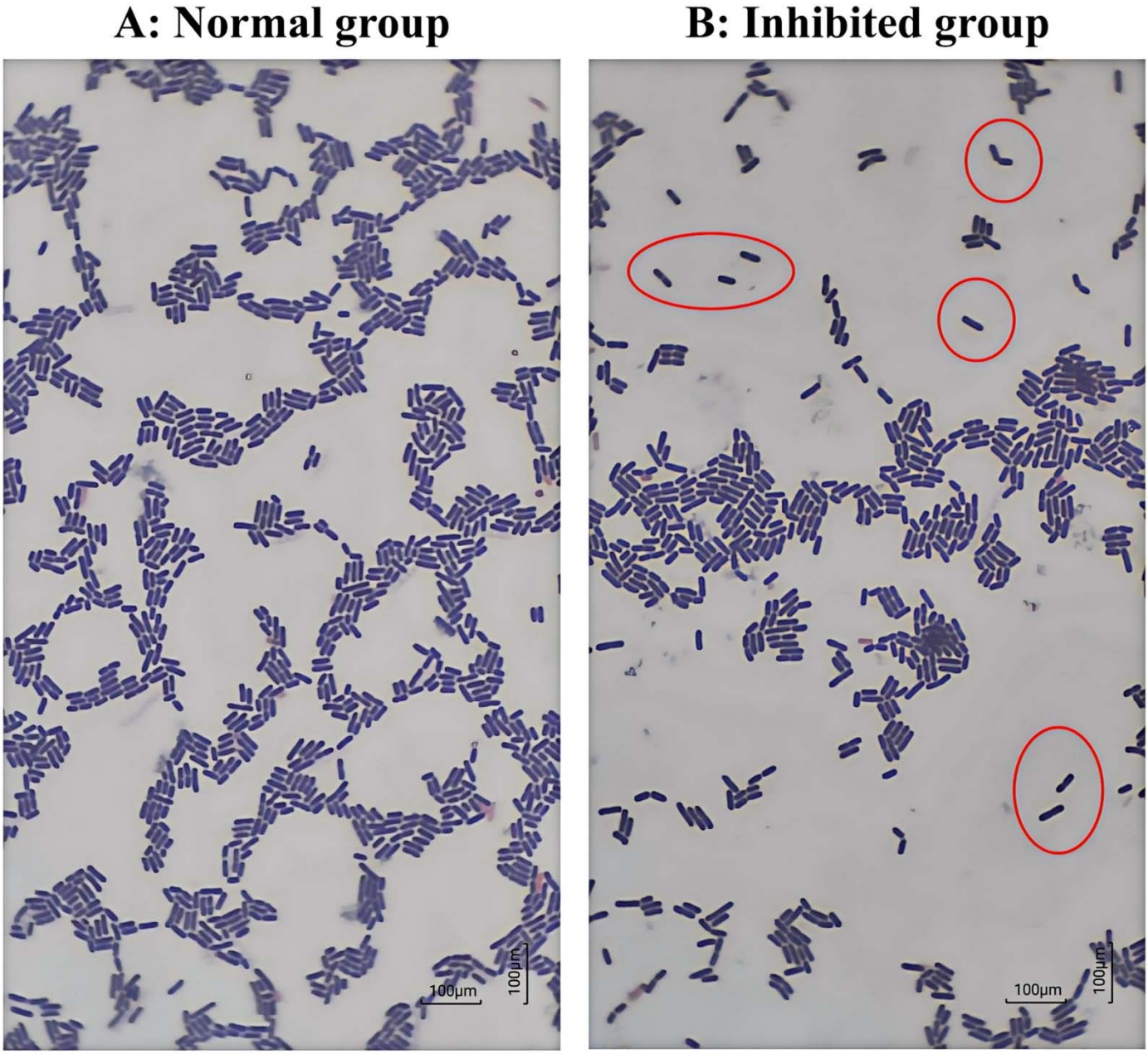

Figure 2. Effects of adding furanone on the mycelial morphology of *L. fermentum* A51.

3.1.2. Effect of adding QSIs on monosaccharide composition of L. fermentum A51 EPS

The above findings demonstrated a decrease in *L. fermentum* A51 EPS yield following the addition of QSIs. However, it remained unclear whether QSIs influenced the monosaccharide composition of EPS. Therefore, the impact of QSIs on the monosaccharide composition of *L. fermentum* A51 EPS was investigated. As illustrated in Fig. 3A, the peak area of each monosaccharide in the inhibited-group was lower than the normal-group, indicating a decrease in the EPS yield of *L. fermentum* A51. Specifically, the EPS yield in the inhibited-group was 196.60 ± 2.53 ug/mg, significantly lower than the 249.50 ± 2.01 ug/mg observed in the normal-group ($P < 0.05$). Additionally, all monosaccharides significantly decreased in the inhibited-group ($P < 0.05$). As illustrated in Fig. 3B, the content of glucose, galactose, mannose,

galacturonic acid and mannose decreased from 130.4 ± 1.6, 67.3 ± 2.4, 30.0 ± 1.5, 16.2 ± 1.6 and 5.7 ± 0.2 ug/mg to 103.5 ± 2.2, 54.6 ± 1.6, 23.00 ± 1.4, 11.3 ± 1.0 and 4.3 ± 0.1 ug/mg, respectively. Interestingly, there was little difference in the molar mass ratio of monosaccharide composition between the normal- and inhibited-groups (Fig. 3C), suggesting that QSIs primarily affected monosaccharide yield than changing their molar mass ratio.

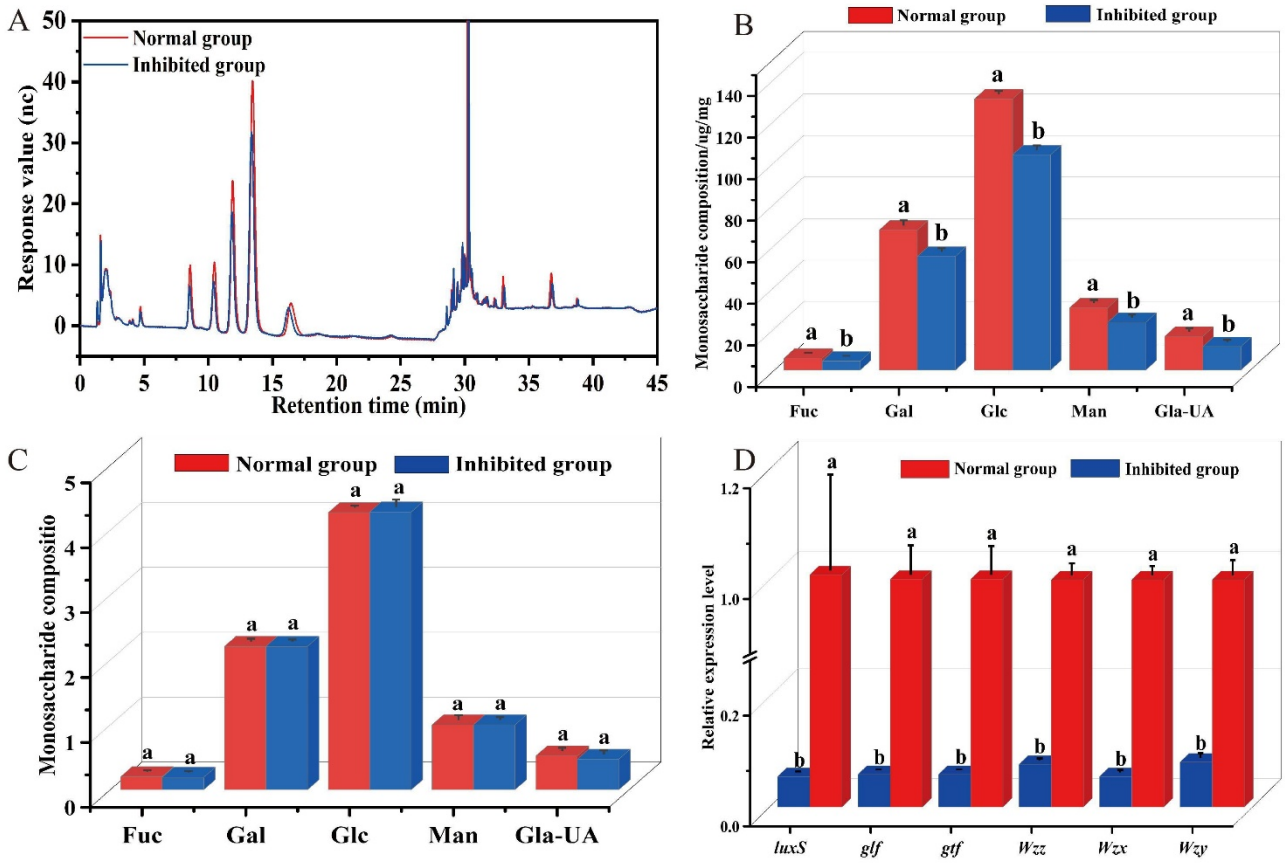

Figure 3. Effects of adding furanone on EPS yield and *eps* gene expression levels in *L. fermentum* A51. (A) HPLC chromatogram of the monosaccharide composition. (B) monosaccharide composition and yield. (C) monosaccharide mass ratio. (D) *eps* gene expression levels. Fuc: fucose; Gal: galactose; Glc: glucose; Man: mannose; Gla-UA: galacturonic acid. Different superscripted lowercase letters indicate $P < 0.05$.

3.1.3. Effect of QSIs on eps genes expression of L. fermentum A51

The effects of QSIs on *eps* gene expression of *L. fermentum* A51 were evaluated, and the results were shown in Fig. 3D. The addition of QSIs significantly inhibited the expression levels of the *eps* genes *glf*, *gtf*, *Wzz*, *Wzx*, *Wzy*, and *luxS* ($P < 0.05$). These findings indicated that the expression of the *luxS* gene was consistent with the *eps* gene, suggesting that AI-2 mediated the EPS biosynthesis of *L. fermentum* A51 at the gene expression level.

3.2. Key proteins and pathways of LuxS/AI-2-QS system-mediated EPS biosynthesis of L. fermentum A51

3.2.1. Protein identification

In order to identify the key proteins and pathways of LuxS/AI-2-QS system mediated EPS biosynthesis of *L. fermentum* A51. We used a TMT-quantitative proteomics strategy to identify differentially abundant proteins in normal- and inhibited-groups, and the results were shown in Fig. 4. Fig. 4A shows the peptide coverage distribution, with > 70% of identified proteins covered by ≥2 unique peptides (dashed line),

meeting rigorous identification criteria. Fig. 4B demonstrates the molecular weight distribution spanning 20-40 kDa, properly representing our protein extraction efficiency across different size ranges. Fig. 4C displays the sequence length distribution, confirming our enzymatic digestion achieved appropriate peptide lengths (6-25 amino acids) for optimal MS detection. A total of 18,583 peptides were generated, and 2,179 proteins were identified, including 2,095 quantifiable proteins (Fig. 5A). Principal component analysis (PCA) was conducted to visually differentiate the sample clusters by comparing the mutual proteins between the normal- and inhibited-groups. The PCA revealed that the first two components accounted for 95.7% of the variability. As illustrated in Fig. 5B, Samples from the two groups could be separated into different quadrants, indicating a significantly different protein profile between the groups. These results suggested that the addition of QSIs affects the physiological activity of *L. fermentum* A51.

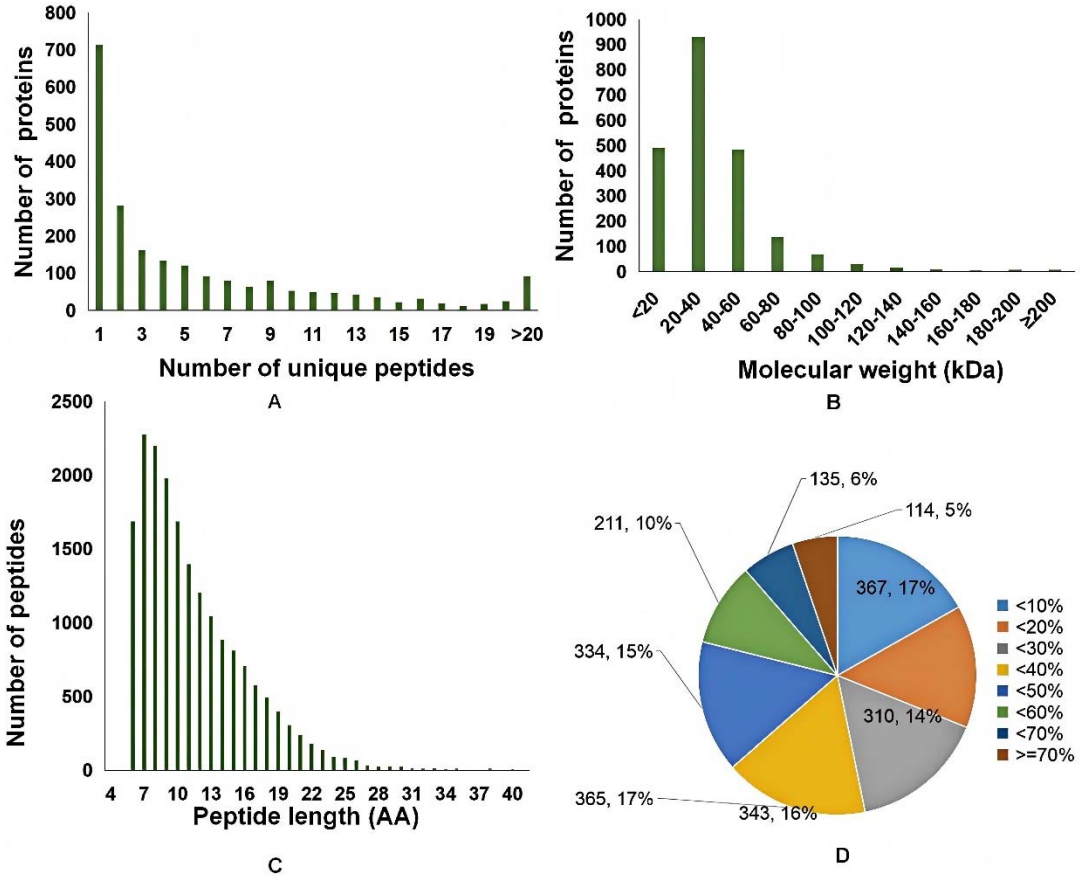

Figure 4. Protein profiling of *L. fermentum* A51 based on TMT-quantitative proteomics analysis. (A) The distribution of peptide number. (B) Statistics on peptide distribution based on molecular weight. (C) Peptide length distribution. (D) Protein coverage distribution plot.

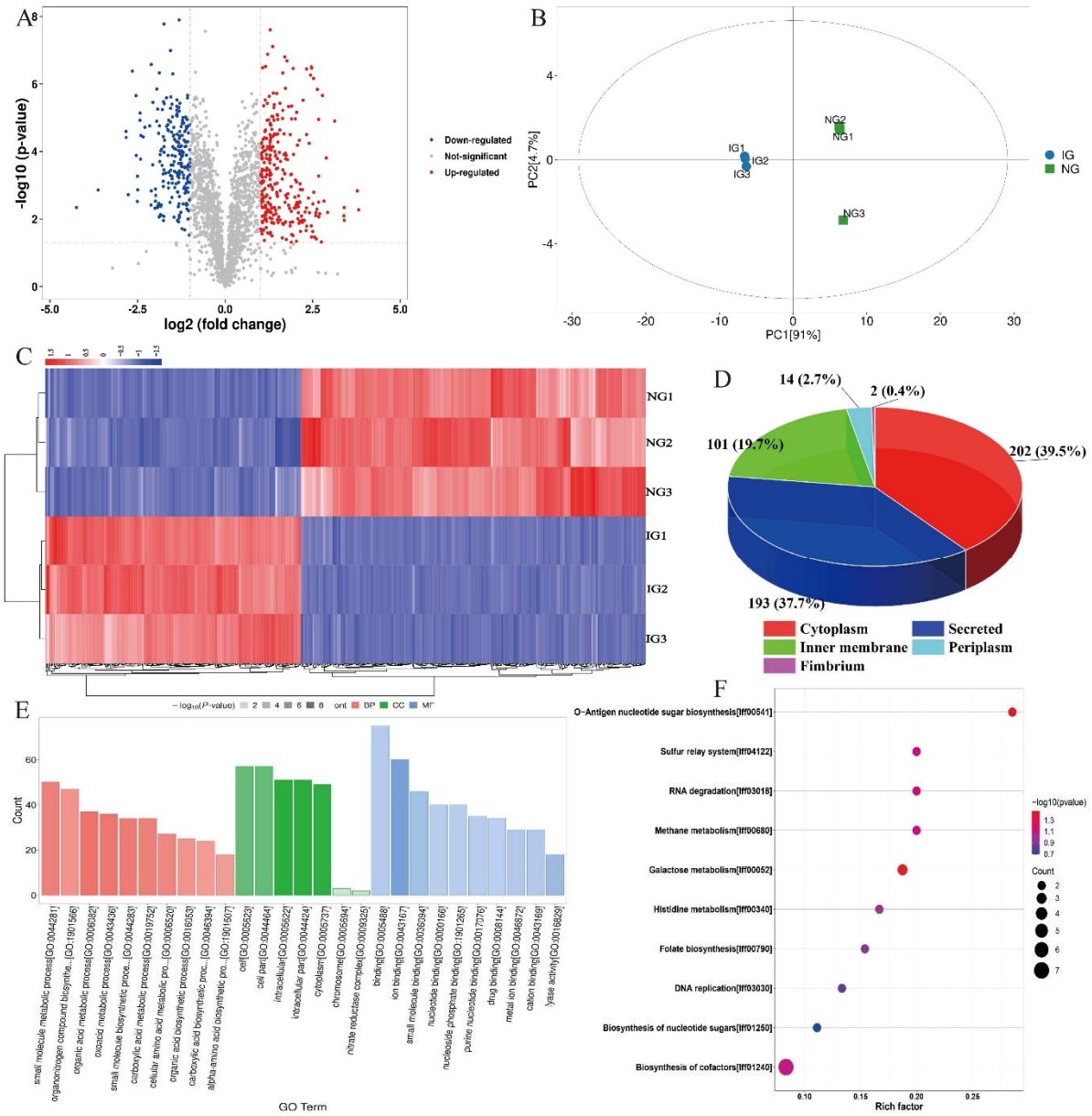

Figure 5. Multivariate statistical analysis of identified *L. fermentum* A51 proteins in the normal- and inhibited-groups. (A) Volcano plot analysis. (B) Principal component analysis. (C) Heat map of clustering of differentially expressed proteins. (D) Subcellular localization of differentially expressed proteins. (E) GO functional annotation analysis of differentially expressed proteins. (F) KEGG functional annotation analysis of differentially expressed proteins. NG: normal-group; IG: inhibited-group.

3.2.2. Differentially expressed proteins (DEPs) and bioinformatics analysis

A total of 512 DEPs were detected in the normal- and inhibited-groups. The expression differences are shown in Fig. 5C, with 294 proteins significantly upregulated and 218 proteins significantly downregulated. We predicted the subcellular localization of these DEPs in *L. fermentum* A51 using the Protein Subcellular Localization Prediction Tool (PSORT). As shown in Fig. 5D, subcellular localization analysis of the DEPs revealed that they were predominantly enriched in the cytoplasm (202, 39.45%), secretory pathway (193, 37.70%), inner membrane (101, 19.73%), periplasm (14, 2.73%), and pilus structures (2, 0.39%). This distribution pattern is consistent with previous reports indicating that, upon QS activation, the DEPs in *L. fermentum* are primarily cytoplasmic [5,8]. Given that the cytoplasm is the primary site of cellular

metabolism, it plays a critical role in QS. Specifically, in Gram-positive bacteria, QS signals are typically perceived by intracellular receptors, and various cytoplasmic enzymes facilitate the synthesis and response to these signaling molecules, thereby regulating intercellular communication [7]. In summary, activation of the QS system in *L. fermentum* A51 significantly alters the expression profiles of cytoplasmic, membrane-associated, and extracellular proteins.

To evaluate the effect of LuxS/AI-2-QS system on the main physiological functions of *L. fermentum* A51, functional and pathway annotation analysis of DEPs was performed using GO and KEGG databases, and the results were shown in Fig. 5E and Fig. 5F. GO annotation analysis showed that DEPs in the molecular functions (MF) category were primarily involved in binding, catalytic activity, and ion binding. DEPs in the cellular component (CC) category were mainly involved with the cell part, intracellular part, and cytoplasm. DEPs in the biological processes category were predominantly involved in cellular process, cellular metabolic process, primary metabolic process, biosynthetic process, organic substance biosynthetic process, and cellular biosynthetic process (Fig. 5E). Additionally, KEGG annotation analysis showed enrichment of DEPs in ten metabolic pathways, including galactose metabolism, RNA degradation, DNA replication, biosynthesis of cofactors, histidine metabolism, folate biosynthesis, and biosynthesis of nucleotide sugars (Fig. 3F).

3.2.3. Key proteins and pathways of LuxS/AI-2-QS system mediated EPS biosynthesis

TMT-quantitative proteomics identified key protein LuxS (A0A4Z0CH58) and AI-2E family transporter (A0A1L7GXS4, A0A158SPH2) involved in the LuxS/AI-2-QS system. This finding suggested that *L. fermentum* A51 secreted the signaling molecule AI-2, which can activate the LuxS/AI-2-QS system [30]. The activation pathway of the LuxS/AI-2-QS system in *L. fermentum* A51 was as follows: First, the LuxS protein regulated the production of AI-2. The AI-2 was then transported extracellularly by the AI-2E transporter. When AI-2 reached a certain concentration threshold, it was internalized into the cell by AI-2-receptor proteins on the membrane [31]. Ultimately, intracellular AI-2 regulated the expression of EPS biosynthesis-related genes and proteins, thus regulating EPS biosynthesis. Notably, among the significantly upregulated proteins, the Putative metal-binding protein (FC = 5.034) and Zinc ribbon domain-containing protein (FC = 4.209) were highlighted. Both proteins are known to play essential roles in signal transduction and metal ion binding, which are often involved in modulating enzymatic activities and cellular responses [32]. Their marked upregulation suggests enhanced intracellular signaling and communication in *L. fermentum* A51 upon activation of the LuxS/AI-2-QS system, which may indirectly influence regulatory networks connected to EPS biosynthesis.

TMT-quantitative proteomics also identified regulatory proteins related to the Wzx/Wzy pathway (Table 2), confirming that the EPS biosynthesis pathway of *L. fermentum* A51 operated via the Wzx/Wzy pathway at the protein level. Based on this pathway and the identified regulatory proteins, the EPS biosynthesis pathway of *L. fermentum* A51 was mapped (Fig. 6). The biosynthesis of EPS in *L. fermentum* A51 involved five main steps. The first step involved lactose, galactose, and glucose phosphorylation and

transportation. Galactose and lactose entered the cytosol via galaclose permease (C0WW47) and lactose permease (A0A2K2TK05), respectively. Lactose entering the cell was broken down to galactose by beta-galactosidase (A0A829LV99) and further phosphorylated by galactokinase (C0WVN4). Meanwhile, lactose and glucose were transferred and phosphorylated by PTS(phosphotransferase system)-lactose and PTS-glucose (A0A158SLW3), respectively. Beta-galactosidase (A0A829LV99) catalyzed the conversion of galactose to phosphor-galactose and phosphor-glucose. The second step in the biosynthesis of EPS in *L. fermentum* A5 involved the production of nucleotides sugar. Glucokinase (A0A4Z0CGL2) and galactose-1-P uridylytransferase (A0A806IVZ1) mediated the conversion of glucose-6-phosphate and galactose-1-phosphate to glucose-1-phosphate, which then transformed into UDP-glucose and UDP-galactose with the aid of different enzymes, including UDP-glucose pyrophosphorylase and UDP-glucose 4-epimerase (A0A0F4HCA3, A0A806IWE9). The third step in the biosynthesis of EPS in *L. fermentum* A5 involved the biosynthesis of repeating units. The biosynthesis of galactose-glucose repeating units at the inner membrane was catalyzed by glycosyltransferases (A0A855ZNS4, A0A829LKR4, A0A0F4HCU9, B2GDK6, B2GDL8, B2GDL1). The fourth step in the biosynthesis of EPS in *L. fermentum* A5 involved the flip of repeating units. The flippase (A0A843R9U2, Wzx) transferred galactose-glucose repeating units to the periplasmic space or outer membrane. The fifth step in the biosynthesis of EPS in *L. fermentum* A5 involved the polymerization and release of galactose-glucose repeating units. The repeating units were polymerized into long chains by polymerase (B2GDM7, Wzy), which were then released into the extracellular space under the regulation of chain-length regulatory proteins. Flippase (Wzx) and polymerase (Wzy) play vital roles in EPS biosynthesis as key members of the Wzx/Wzy pathway [33].

Table 2. Differentially expressed proteins involved in LuxS/AI-2-QS system and Wzx/Wzy pathway.

NO	Gene Name	Accession	Description	FC Value	Threshold
1	LuxS	A0A4Z0CH58	S-ribosylhomocysteine lyase	2.233	Up
2	AI-2E	A0A1L7GXS4	AI-2 export family transporter	1.910	Up
3	AI-2E	A0A158SPH2	AI-2 export family transporter	1.424	Up
4	C1Y38_02970	A0A2K2TK05	Lactose permease	1.157	Up
5	HMPREF0511_1672	C0WZX1	ABC transporter, substrate-binding protein, family 3	2.614	Up
6	LAF_1168	B2GCX2	Amino acid ABC transporter substrate-binding component	1.988	Up
7	LF130101_279	A0A2N8Z2G0	Putative metal-binding protein	5.034	Up
8	LBFF_1105	A0A806IUA5	Amino acid ABC superfamily ATP binding cassette transporter substrate binding protein	2.374	Up
9	GDZ34_03130	A0A843R6Z4	Zinc ribbon domain-containing protein	4.209	Up
10	HMPREF05110348	C0WW47	Galaclose Permease	1.701	Up
11	LFER_1540	A0A158SNJ0	PTS system galactitol-specific IIC component	1.495	Up
12	treB	A0A158SLW3	PTS system, beta glucosides specific IIA component	1.941	Up
13	NB22_02610	A0A829LV99	Beta-galactosidase	1.542	Up
14	N573_011175	A0A806TYB1	Alpha-galactosidase	3.842	Up
15	LBFF_1972	A0A806IK59	Alpha-galactosidase	4.865	Up
16	galK	C0WVN4	Galactokinase	0.806	Down
17	LAF_0350	B2GAK4	Phosphoglucomutase	0.644	Up
18	galT	A0A806IVZ1	Galactose-1-phosphate uridylyltransferase	1.169	Up
19	galE	A0A0F4HCA3	UDP-glucose 4-epimerase	1.263	Up

NO	Gene Name	Accession	Description	FC Value	Threshold
20	galE3	A0A806IWE9	UDP-glucose 4-epimerase	3.615	Up
21	glf	A0A806IIM8	UDP-galactopyranose mutase	1.376	Up
22	gk	A0A4Z0CGL2	Glucokinase	1.311	Up
23	gtf	A0A855ZNS4	Glycosyl transferase	2.162	Up
24	gtf	A0A829LKR4	Glycosyl transferase	2.440	Up
25	gtf	A0A0F4HCU9	Glycosyl transferase	1.829	Up
26	gtf	B2GDK6	Glycosyl transferase	1.998	Up
27	gtf	B2GDL8	Glycosyl transferase	1.283	Up
28	gtf	B2GDK9	Glycosyl transferase	1.830	Up
29	HMPREF0513_00637	D0DSJ8	Glycosyltransferase, group 2 family protein	2.241	Up
30	Wzx	A0A843R9U2	Flippase	1.959	Up
31	Wzy	B2GDM7	Polymerase	2.182	Up
32	Wzd	A0A829M0M2	Capsular polysaccharide biosynthesis protein CpsC	1.796	Up

Note: FC, Fold Change; Fold Change > 1 means up, Fold Change < 1 means down; Up means upregulated, Down means downregulated.

The differential expression of key regulatory proteins in the normal- and inhibited-groups was compared to clarify the regulatory relationship between the LuxS/AI-2-QS system and the Wzx/Wzy pathway. The expression levels of LuxS/AI-2-QS system and Wzx/Wzy pathway related regulatory proteins were significantly decreased in the inhibited-group compared with the normal-group (except for C0WVN4), indicating that the addition of QSIs inhibited the activity of both the LuxS/AI-2-QS system and the Wzx/Wzy pathway (Table 2). These results further demonstrated that the LuxS/AI-2-QS system regulated the EPS biosynthesis of *L. fermentum* A51 by mediating the Wzx/Wzy pathway at the protein expression level.

3.3. Verification of key regulatory proteins by PRM

PRM can detect specific proteins with high sensitivity and resolution, commonly used for quantitative identification of regulatory proteins [34-36]. The TMT-proteomics data was validated by selecting 32 candidate DEPs closely related to the LuxS/AI-2-QS system and EPS biosynthesis for further PRM protein targeting validation. Among these candidates, only twelve DEPs were successfully validated, including LuxS/AI-2-QS system-related proteins (A0A4Z0CH58 and A0A1L7GXS4) and Wzx/Wzy pathway related proteins (A0A0F4HCA3, B2GDK6, B2GDK9, B2GDL8, A0A806IVZ1, A0A4Z0CGL2, A0A843R9U2, B2GDM7, and A0A806IK59) (Table 3). However, only twelve DEPs identified through TMT analysis were validated in PRM analysis. The reason for this outcome is that PRM validation fundamentally relies on the detection and quantification of specific and unique peptides to achieve reliable quantitative analysis of proteins. However, some candidate proteins lack suitable unique peptides that can be unequivocally targeted, or the targeted peptides are not amenable to PRM validation due to low natural abundance, insufficient ionization efficiency, or other matrix effects [37]. The expression patterns of these proteins showed similar trends between the quantitative results of PRM and TMT, supporting the reliability of the TMT data. The abundance of both LuxS/AI-2-QS system and EPS biosynthesis-related proteins decreased after treatment with the QSIs (except for A0A0F4HCA3 and A0A4Z0CGL2) compared to the normal-group, indicating inhibition of the LuxS/AI-2-QS system and the Wzx/Wzy pathway. In particular, A0A1L7GXS4 (AI-2E)

and A0A806IVZ1 (galT) showed the highest fold changes (FCs) of 17.381 and 11.132, respectively, followed by A0A806IK59, A0A843R9U2 (Wzx), B2GDM7 (Wzy), B2GDK9, and A0A4Z0CH58 (LuxS) with FCs of 7.353, 2.801, 3.401, 2.582, and 1.925, respectively.

Table 3. PRM validates key regulatory proteins.

Gene Name	Accession	Peptide Sequence	Description	FC value TMT NG/IG	PRM NG/IG
LuxS	A0A4Z0CH58(LuxS)	EAGVSTTTVSR	S-ribosylhomocysteine lyase	2.233	1.925
AI-2E	A0A1L7GXS4(AI-2E)	LLLTTYLPGQVAR	AI-2 export family transporter	1.91	17.381
HMPREF0511_1672	C0WZX1(AI-2R)	QKSGELDKLFKKAQE	ABC transporter, substrate-binding protein, family 3	2.614	4.622
galE	A0A0F4HCA3(galE)	YDDVHDIIATAWK	UDP-glucose 4-epimerase	1.263	0.448
gtf	B2GDK6	SGQNLGGSGGFSNAIR	Glycosyl transferase	1.998	2.702
gtf	B2GDL8	DLIDNLGLIFDTSLK	Glycosyl transferase	1.283	1.962
gtf	B2GDK9	LNTFSDGFK	Glycosyltransferase	1.830	2.584
galT	A0A806IVZ1(galT)	IAPAHLSWAQEVASR	Galactose-1-phosphate uridylyltransferase	1.169	11.132
E2P75_07395	A0A4Z0CGL2	FLVIGGGVSAAGVFLLKRV	Glucokinase	1.311	0.823
Wzx	A0A843R9U2(Wzx)	PWFLGNGYQDAGKIIFFEAP	Flippase	1.959	2.801
Wzy	B2GDM7(Wzy)	QQLYLLGFTYFFTIAFLQTSM	Polymerase	2.182	3.401
LBFF_1972	A0A806IK59	YTIFNNYNAIAR	Alpha-galactosidase	4.865	7.353

Note: NG, normal-group, IG, inhibited-group; FC, Fold Change; Fold Change > 1 means up, Fold Change < 1 means down.

4. Discussion

LAB-EPS are known for their viscous properties and are widely used in the food industry to improve viscosity, flavor, and texture [10]. Additionally, EPS exhibit diverse biological activities, making them promising for probiotic product development [11]. Although the LuxS/AI-2-QS system has been reported to mediate the biosynthesis of functional components in LAB [2,6,8], its regulatory role in EPS formation remains inadequately explored. In previous studies, we isolated a strain of *L. fermentum* A51, which yields a high amount of EPS, and successfully applied it in yogurt production [24]. We also observed a positive correlation between AI-2 activity and EPS yield [25]. However, the specific regulatory mechanisms linking the LuxS/AI-2 system to EPS biosynthesis remain unclear and require further elucidation.

To elucidate the regulatory relationship between the LuxS/AI-2-QS system and EPS biosynthesis in *L. fermentum* A51, we investigated the effects of adding QSIs on EPS biosynthesis. The addition of QSIs did not affect the growth of *L. fermentum* A51. However, it significantly inhibited AI-2 activity and EPS yield, and reduced strain adhesion ($P < 0.05$). During the initial phase of cultivation, the concentration of AI-2 signaling molecules synthesized by the strain remained low, failing to reach the activation threshold of the QS system. Consequently, the regulatory mechanism governing EPS synthesis was not initiated. As the incubation period extended, AI-2 gradually accumulated in the normal-group, successfully activating the LuxS/AI-2 pathway and significantly promoting EPS production. In contrast, the inhibited-group exhibited

suppressed AI-2 synthesis, preventing effective activation of this pathway and resulting in significantly lower EPS yields compared to the normal-group [5]. There are three known pathways by which QSIs inhibit the QS system: inhibiting the generation of signaling molecules, hindering the binding of signaling molecules to receptor proteins, and degrading the signaling molecules. AI-2, a furan analog, shares structural homology with furanone compounds [38]. The exogenously supplemented furanone competitively binds to AI-2-specific membrane receptor proteins, thereby blocking extracellular AI-2 uptake. As the intracellular AI-2 concentration dropped below the critical threshold, the LuxS/AI-2-QS system was effectively suppressed, leading to attenuated AI-2 biosynthesis and subsequent reduction in QS-mediated activity [39]. Inhibition of the LuxS/AI-2-QS system led to decreased total EPS, monosaccharide yield, and adhesion of *L. fermentum* A51, which indicated that LuxS/AI-2-QS system activity positively correlated with EPS yield. These findings were consistent with previous studies by Wang et al. [14] and Zheng et al. [40], suggesting that QSIs affected the aggregation ability of the *L. fermentum* and reduced biofilm (primarily composed of EPS) formation. Based on these findings, it is reasonable to deduce that the LuxS/AI-2-QS system mediated the EPS biosynthesis of *L. fermentum* A51.

Further investigations revealed that the addition of QSIs resulted in the downregulation of both *luxS* and *eps* genes. This finding indicated that the expression of the *luxS* gene was consistent with that of the *eps* gene, suggesting that AI-2 mediated the EPS biosynthesis of *L. fermentum* A51 at the gene expression level. Previous studies have demonstrated that the EPS produced by *L. fermentum* A51 was a heteropolysaccharide (HePS) composed of fucose, galactose, glucose, mannose, and galacturonic acid [24]. The Wzx/Wzy pathway is considered the main pathway for the biosynthesis of HePS. This pathway can be divided into two steps: the biosynthesis of nucleotide sugar and the assembly and polymerization of polysaccharides [11]. Quantitative PCR identified *eps* genes, including *glf*, *gtf*, *Wzz*, *Wzx*, and *Wzy*. These genes were enriched in the Wzx/Wzy pathway, suggesting that the EPS biosynthesis pathway of *L. fermentum* A51 was Wzx/Wzy pathway. Notably, the *glf* gene was mainly involved in the biosynthesis of EPS precursor sugar ribonucleotides. The *gtf* gene encodes a glycosyltransferase, which transfers sugar ribonucleotides to lipid carriers in the intracellular membrane [31]. The *Wzz* gene regulates the biosynthesis of chain-length regulatory proteins and controls the length of polysaccharide chains by controlling the number of repetitive units added. The *Wzx* gene encodes a flippase, which transfers repetitive units to the periplasmic space of the cell or the outer membrane. Lastly, the *Wzy* gene encodes a polymerase, which merges short-chained repetitive units into long-chained polymers. This genetic architecture is consistent with functional studies in related bacteria. For instance, Kong et al. [18] demonstrated that CRISPR/nCas9-mediated knockout of *epsC (Wzz)*, *epsE (gtf)*, and *epsG (gtf)* in *Streptococcus thermophilus* S-3 significantly altered EPS production, molecular weight, monosaccharide composition, and viscosity, underscoring the critical roles of these genes in EPS biosynthesis. This highlights the essential roles of these genes in EPS biosynthesis. Collectively, our findings indicate that *glf*, *gtf*, *Wzz*, *Wzx,* and *Wzy* are key genetic determinants of EPS synthesis in *L. fermentum* A51. Furthermore, the concordant downregulation of *luxS* and these *ep*s genes in response to

QSIs suggests that the LuxS/AI-2-QS system modulates EPS biosynthesis through transcriptional regulation of the Wzx/Wzy pathway.

We then quantitatively compared differentially abundant proteins of *L. fermentum* A51 between the normal- and inhibited-groups using TMT-proteomics. A total of 512 DEPs were identified between the normal- and inhibited-groups, with 294 upregulated and 218 downregulated proteins. GO and KEGG annotations revealed that DEPs were primarily enriched in galactose metabolism, nucleotide sugar biosynthesis, primary metabolism, organic substance biosynthesis, and DNA replication. The inhibition of the LuxS/AI-2-QS system affected the expression of transporter proteins in *L. fermentum* A51, reducing the levels of substances and energy transport and signaling exchange. This effect ultimately impacted the expression of genetic information, galactose metabolism, nucleotide sugar biosynthesis, and information exchange within the strain. Thus, we hypothesized that QSIs may affect key proteins involved in the transport and metabolism of carbohydrates and coenzymes in *L. fermentum* A51, thus affecting EPS formation.

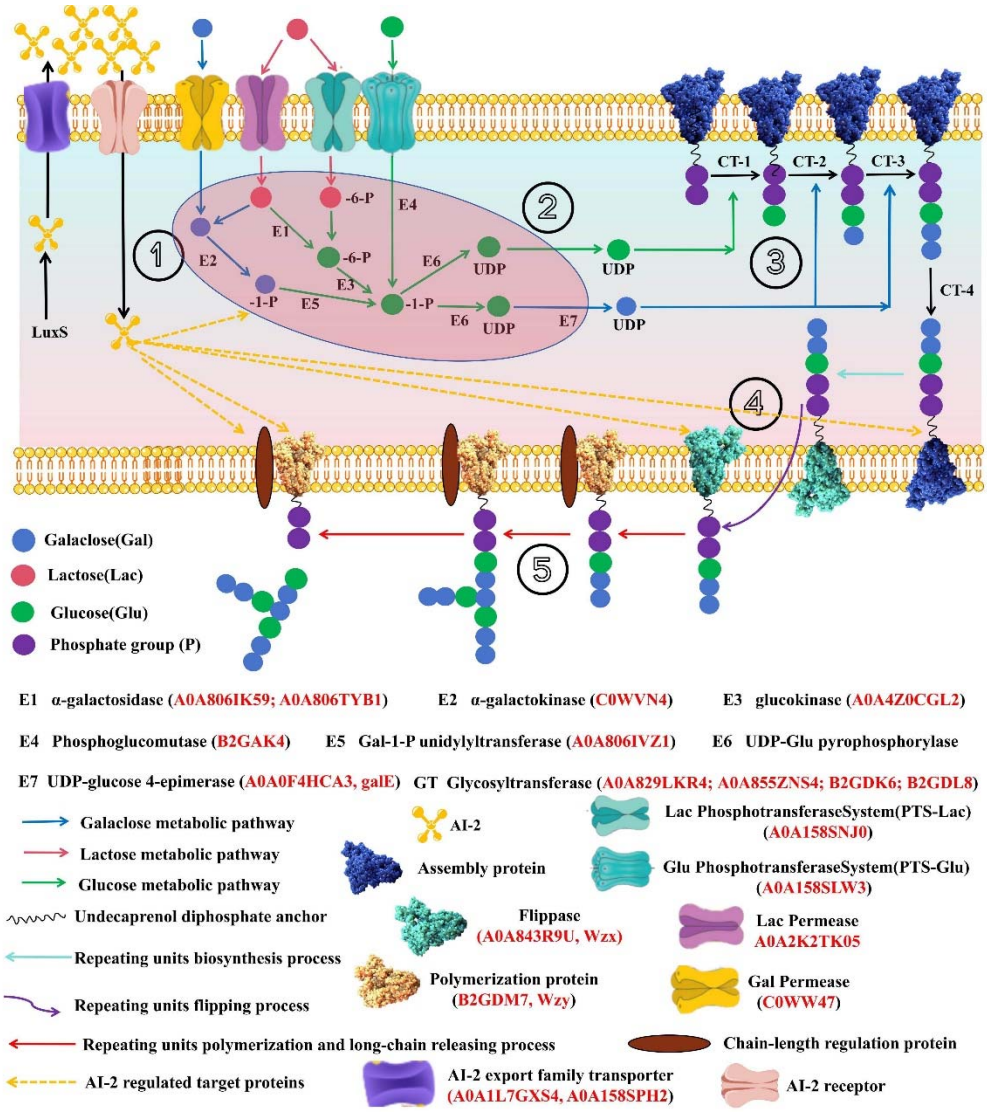

Figure 6. Schematic diagram key regulatory proteins of the LuxS/AI-2-QS system regulating EPS biosynthesis in *L. fermentum* A51. The ①②③④⑤ represent the five steps in the EPS synthesis: ① Monosaccharide and disaccharides phosphorylation or transportation;② The production of sugar nucleotides; ③ The biosynthesis of repeating units; ④ The transfer position of repeating units; ⑤ The polymerization and export of long chains.

TMT quantitative proteomics identified key proteins associated with the LuxS/AI-2-QS system and EPS biosynthesis. Then, the EPS biosynthesis pathway of *L. fermentum* A51 was mapped based on the known Wzx/Wzy pathway and the identified regulatory proteins, and the results were shown in Fig. 6. The expression levels of key regulatory proteins were consistent in the normal- and inhibited-groups, indicating that the LuxS/AI-2-QS system regulated EPS biosynthesis in *L. fermentum* A51 by mediating the Wzx/Wzy pathway. The biosynthesis of EPS through the Wzx/Wzy pathway involved several regulatory proteins. Whether the LuxS/AI-2-QS system regulated EPS biosynthesis by influencing the expression of proteins related to the production of glycanucleotides or polysaccharide polymerization and assembly in the Wzx/Wzy pathway requires further investigation. Previous studies have shown that AI-2 affected the biofilm formation of *L. plantarum* L-ZS9 by regulating the expression of cell membrane proteins and membrane transporter proteins, such as the LacI, AraC, and PadR family proteins) [39,41]. Additionally, AI-2 influenced biofilm formation in *Bifidobacterium* by regulating the expression of transmembrane transporter proteins RbsA, RbsB, and RbsC [42]. Similarly, our data suggest that Wzx and Wzy may be key membrane targets of AI-2 signaling in *L. fermentum* A51. Therefore, we hypothesized that the LuxS/AI-2-QS system may affect EPS biosynthesis of *L. fermentum* by regulating the expression of membrane proteins such as Wzx and Wzy.

The twelve key proteins verified by PRM were integrated into the schematic diagram of LuxS/AI-2-QS system regulating EPS biosynthesis (Fig. 6). Furthermore, the mechanism of LuxS/AI-2-QS system-mediated Wzx/Wzy pathway regulation of EPS biosynthesis was summarized in Fig. 7. The regulatory mechanism was as follows: AI-2, synthesized by the LuxS protein, was transported extracellularly by the transporter protein AI-2E. When the extracellular AI-2 concentration reached a certain threshold, it was recognized by the AI-2 receptor protein and internalized into the cell. The accumulated intracellular AI-2 then initiates a signaling response, ultimately leading to the upregulation of key components within the Wzx/Wzy pathway. Although the precise molecular linkages require further validation, the intracellular AI-2 signal is likely recognized by homologs of the LuxR or LuxB protein families, triggering a phosphorylation cascade [2]. This cascade would directly or indirectly enhance the transcription of the *Wzx* and *Wzy* genes, thereby promoting EPS assembly and secretion. When the Wzx/Wzy pathway was activated, the expression of proteins related to glycanucleotides biosynthesis regulation (B2GDK6, B2GDK9, B2GDL8, A0A806IK59, and A0A806IVZ1) also increased. However, the addition of QSIs competed with AI-2 for receptor proteins, resulting in a decrease in the amount of AI-2 entering the intracellular compartment. When the intracellular AI-2 concentration was below the threshold, the LuxS/AI-2-QS system and the Wzx/Wzy pathway were inhibited, downregulating the expression of proteins LuxS, AI-2E, AI-2R, Wzx, and Wzy, which in turn decreased AI-2 activity and EPS yield. These newly identified key regulatory proteins are suitable targets for future regulation of EPS biosynthesis. In summary, incorporating biochemical, proteomics, and PRM technologies was effective for elucidating the underlying mechanisms of the LuxS/AI-2-QS system in regulating EPS biosynthesis in LAB. To the best of our knowledge, this study provides the first direct evidence that the LuxS/AI-2-QS system specifically

regulates EPS biosynthesis in LAB through mediation of the Wzx/Wzy pathway, establishing a clear mechanistic link beyond previous reports of LuxS/AI-2-QS system involvement. Future studies should aim to validate the identified regulatory nodes through genetic engineering and explore the broader applicability across diverse LAB strains and QS systems. Additionally, employing a wider array of QSIs and investigating the crosstalk with other regulatory networks would provide a more comprehensive understanding. Ultimately, the corresponding coding genes of these key proteins, such as those within the Wzx/Wzy pathway, can be precisely modulated using CRISPR/Cas9-based gene editing. This strategy holds significant promise for achieving high and tailored EPS production in Lactobacillus, thereby promoting its advanced application in the food industry for texture modification, bio-thickening, or developing novel functional foods.

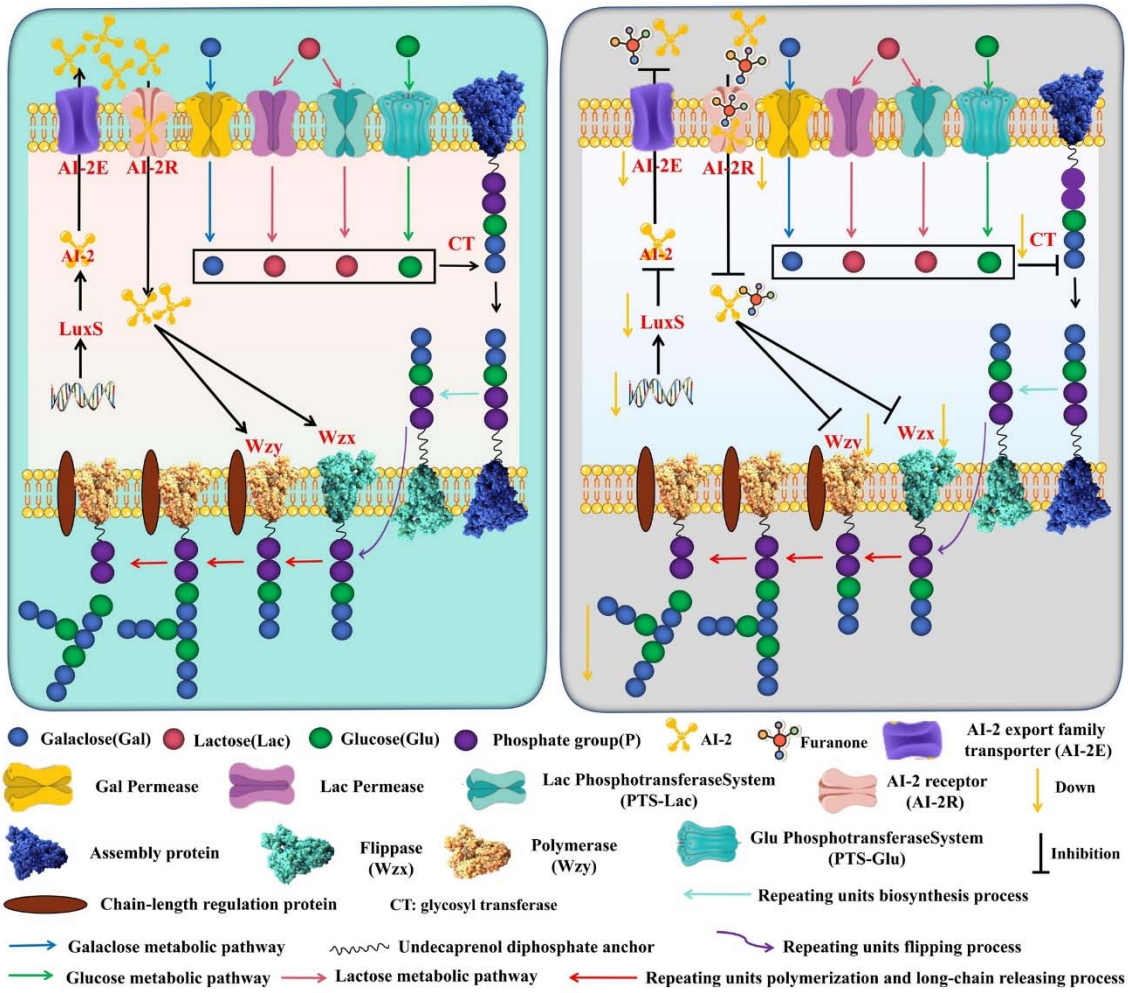

Figure 7. The regulatory mechanism of the LuxS/AI-2-QS system on EPS biosynthesis of *L. fermentum* A51 mediated by the Wzx/Wzy pathway. The dark green area represents the normal state, and the grey area represents the inhibited state.

5. Conclusions

This study was the first to reveal the regulatory mechanism of the LuxS/AI-2-QS system on EPS biosynthesis in LAB. We found that *luxS* gene and protein expression were consistent with AI-2 activity and positively correlated with *eps* genes, protein expression, EPS yield, and strain adhesion. Our results demonstrated that the LuxS/AI-2-QS system mediates EPS biosynthesis in *L. fermentum* A51 at the gene and protein expression levels. Additionally, twelve key regulatory proteins were validated using proteomics

coupled with PRM technology. Further mechanistic analysis revealed that the LuxS/AI-2-QS system regulates EPS biosynthesis in *L. fermentum* A51 by activating the Wzx/Wzy pathway by up-regulation of the expression of the glycosyl transferase, galactose-1-phosphate uridylyltransferase, glucokinase, Wzx and Wzy. Future studies should further validate the key regulatory proteins by western blot. These findings advance our understanding of the LuxS/AI-2-QS system's mechanism in regulating EPS biosynthesis and provide new insights into the efficient and stable regulation of EPS production by LAB.

Declaration of competing interest

The authors declare that no conflict of interest in this work.

Acknowledgements

This study was financially supported by the Yunnan Provincial Department of Education Project (Grant No. 2025J0360), the Recognition of International Science and Technology Commissioners (Individual) in Yunnan Province (No. 202503AK140027), the National Natural Science Foundation of China (No. 32260578), the Yunling Scholar Program (grant No. XDYC-YLXZ-2023-0032).

References

[1] D. Wang, H. Xiang, D. Sun-Waterhouse, et al., Autoinducer-2-mediated quorum sensing promotes histamine formation by *Morganella psychrotolerans*, Food Science and Human Wellness, 1-14. https://link.cnki.net/urlid/10.1750.TS.20250509.1035.016.

[2] F. Meng, M. Zhao, Z. Lu, The LuxS/AI-2 system regulates the probiotic activities of lactic acid bacteria, Trends Food Sci. Technol. 127 (2022) 272-279, https://doi.org/10.1016/j.tifs.2022.05.014.

[3] Y. Gu, B. Zhang, J. Tian, et al., Physiology, quorum sensing, and proteomics of lactic acid bacteria were affected by *Saccharomyces cerevisiae* YE4, Food Res. Int. 166 (2023) 112612, https://doi.org/10.1016/j.foodres.2023.112612.

[4] J. Liu, D. Liu, Z. Hu, et al., TMT quantitative proteomics analysis reveals molecular mechanism of ferroptosis during beef refrigeration, Food Chem. 435 (2024) 137596, https://doi.org/10.1016/j.foodchem.2023.137596.

[5] Q. Ma, Y. Chai, Z. Yang, et al., Deciphering the mechanisms of *Limosilactobacillus fermentum* L1 involved in conjugated linoleic acid regulated by LuxS/AI-2 quorum sensing, LWT 154 (2022) 112736, https://doi.org/10.1016/j.lwt.2021.112736.

[6] J. E., R. Ma, Z. Chen, et al., Improving the freeze-drying survival rate of *Lactobacillus plantarum* LIP-1 by increasing biofilm formation based on adjusting the composition of buffer salts in medium, Food Chem. 338 (2021) 128134, https://doi.org/10.1016/j.foodchem.2020.128134.

[7] Y. Chai, Q. Ma, X. Nong, et al., Dissecting LuxS/AI-2 quorum sensing system-mediated phenyllactic acid production mechanisms of *Lactiplantibacillus plantarum* L3, Food Res. Int. 166 (2023) 112582, https://doi.org/10.1016/j.foodres.2023.112582.

[8] Y. Chai, W. Zheng, S. Hu, et al., Novel molecular mechanisms of gamma-aminobutyric acid production mediated by LuxS/AI-2 quorum sensing system in *Limosilactobacillus fermentum* B41, Int. J. Food Microbiol. 439 (2025) 111269, https://doi.org/10.1016/j.ijfoodmicro.2025.111269.

[9] Y. Zhang, H. Zhong, Y. Zheng, et al., Use of whole-genome analysis to study the effect of various quorum-sensing inhibitors on the biofilm formation of *Lactobacillus fermentum*, LWT-Food Sci Technol 173 (2023) 114378, https://doi.org/10.1016/j.lwt.2022.114378.

[10] K. Evelin, V. László, Exopolysaccharides from lactic acid bacteria: techno-functional application in the food industry, Trends Food Sci. Technol. 110 (2021) 375-384, https://doi.org/10.1016/j.tifs.2021.02.014.

[11] J. Wu, X. Han, M. Ye, et al., Exopolysaccharides synthesized by lactic acid bacteria: biosynthesis pathway, structure-function relationship, structural modification and applicability, Crit. Rev. Food Sci. Nutr. 63 (2022) 21-22, https://doi.org/10.1080/10408398.2022.2043822.

[12] Y. Ji, The effects of environmental stress on the production of biofilm, signal molecule AI-2 and eps in lactic acid bacteria[D], Inner Mongolia Agricultural University, 2020. https://doi.org/10.27229/d.cnki.gnmnu.2020.000944.

[13] R. Wu, Effect of signal molecule AI-2 on biofilm formation of lactic acid bacteria[D], Inner Mongolia Agricultural University, Hohhot, 2018.

[14] Y. Wang, Y. Gu, Y. Zhang, et al., Effects of exogenous AI-2 on extracellular polysaccharide producted by *Lactobacillus fermentum* TG4-1-1 and *Pediococcus acidilactici* 11-3, J. Chin. Inst. Food Sci. Technol. 23 (2023) 18-28, https://doi.org/10.16429/j.1009-7848.2023.06.003.

[15] Y. Zhang, Y. Gu, Y. Zheng, et al., Deletion of *luxS* gene mediated by λred gene recombination technology reduces biofilm formation and stress resistance of *Lactobacillus fermentum*, Food Biosci. 49 (2022) 101892, https://doi.org/10.1016/j.fbio.2022.101892.

[16] A. Zeidan, K. Poulsen, T. Janzen, et al., Polysaccharide production by lactic acid bacteria: from genes to industrial applications, FEMS Microbiol. Rev. 41 (2017) 168-200, https://doi.org/10.1093/femsrefux017.

[17] Y. Zhou, Y. Cui, X. Qu, Exopolysaccharides of lactic acid bacteria: structure, bioactivity and associations: a review, Carbohydr. Polym. 207 (2019) 317-332, https://doi.org/10.1016/j.carbpol.2018.11.093.

[18] L. Kong, X. Song, Y. Xia, et al., Construction of a CRISPR/nCas9-assisted genome editing system for exopolysaccharide biosynthesis in *Streptococcus thermophilus*, Food Res. Int. 158 (2022) 111550, https://doi.org/10.1016/j.foodres.2022.111550.

[19] Z. Zhang, Q. Xu, M. Gou, et al., Potential mechanism of improved cryotolerance of *Pediococcus pentosaceus* YT2 cold acclimation based on tmt quantitative proteomics analysis, LWT-Food Sci. Technol. 192 (2024) 115714, https://doi.org/10.1016/J.lwt.2023.115714.

[20] S. Gallien, E. Duriez, C. Crone, et al., Targeted proteomic quantification on quadrupole-orbitrap mass spectrometer, Mol. Cell Proteomics 11 (2012) 1709-1723, https://doi.org/10.1074/mcp.O112.019802.

[21] A.C. Peterson, J.D. Russell, D.J. Bailey, et al., Parallel reaction monitoring for high resolution and high mass accuracy quantitative, targeted proteomics, Mol. Cell Proteomics Mcp 11 (2012) 1475-1488, https://doi.org/10.1074/mcp.O112.020131.

[22] A. Bourmaud, S. Gallien, B. Domon, Parallel reaction monitoring using quadrupole-orbitrap mass spectrometer: principle and applications, Proteomics 16 (2016) 2146-2159, https://doi.org/10.1002/pmic.201500543.

[23] E. Borràs, E. Sabidó, What is targeted proteomics a concise revision of targeted acquisition and targeted data analysis in mass spectrometry, Proteomics 17 (2017) 17-18, https://doi.org/10.1002/pmic.201700180.

[24] G. Wei, X. Dai, B. Zhao, et al., Structure-activity relationship of exopolysaccharides produced by *Limosilactobacillus fermentum* A51 and the mechanism contributing to the textural properties of yogurt, Food Hydrocoll. 144 (2023) 108993, https://doi.org/10.1016/J.foodhyd.2023.108993.

[25] G. Wei, D. Wang, T. Wang, et al., Probiotic potential and safety properties of *Limosilactobacillus fermentum* A51 with high exopolysaccharide production, Front. Microbiol. 16 (2025) 1498352, https://doi.org/10.3389/fmicb.2025.1498352.

[26] C. Wu, T. Lin, Y. Wu, et al., Inhibitory effect of *Lactobacillus salivarius* on streptococcus mutans biofilm formation, Mol. Oral Microbiol. 30 (2015) 16-26, https://doi.org/10.1111/omi.12063.

[27] L. Wang, B. Zhang, J. Xiao, et al., Physicochemical, functional, and biological properties of water-soluble polysaccharides from rosa roxburghii tratt fruit, Food Chem. 249 (2018) 127-135, https://doi.org/10.1016/j.foodchem.2018.01.011.

[28] W. Ma, D. Zhang, G. Li, et al., Antibacterial mechanism of daptomycin antibiotic against staphylococcus aureus based on a quantitative bacterial proteome analysis, J. Proteomics 150 (2017) 242-251, https://doi.org/10.1016/j.jprot.2016.09.014.

[29] Y. Chai, C. Zi, G. Wei, et al., Molecular mechanisms of high aldehyde dehydrogenase production for improved beany flavour regulated by the LuxS/AI-2 quorum sensing system in *Limosilactobacillus fermentum* A119, LWT 207 (2024) 116674, https://doi.org/10.1016/J.lwt.2024.116674.

[30] D. Duanis-Assaf, D. Steinberg, Y. Chai, et al., The *luxS* based quorum sensing governs lactose induced biofilm formation by bacillus subtilis, Front. Microbiol. 6 (2015) 1517, https://doi.org/10.3389/fmicb.2015.01517.

[31] Y. Zhang, K. Qi, Y. Jing, et al., Lsrb-based and temperature-dependent identification of bacterial AI-2 receptor, AMB Express 7 (2017) 188, https://doi.org/10.1186/s13568-017-0486-y.

[32] X. Zeng, T. Wei, X. Wang, et al. Discovery of metal-binding proteins by thermal proteome profiling. Nat. Chem. Biol. 20 (2024) 770-778, https://doi.org/10.1038/S41589-024-01563-Y.

[33] C. Hidalgo-Cantabrana, P. López, M. Gueimonde, et al., Immune modulation capability of exopolysaccharides synthesised by lactic acid bacteria and bifidobacteria, Probiotics & Antimicrobial Proteins 4 (2012) 227-237, https://doi.org/10.1007/s12602-012-9110-2.

[34] Z. Gao, Q. Liu, Y. Zhang, et al., Oscul3a-associated molecular switches have functions in cell metabolism, cell death, and disease resistance, J. Agric. Food. Chem. 68 (2020) 5471-5482, https://doi.org/10.1021/acs.jafc.9b07426.

[35] C. Tang, Y. Xu, D. Yu, et al., Label-free quantification proteomics reveals potential proteins associated with the freshness status of crayfish (Procambarus clarkii) as affected by cooking, Food Res. Int. 160 (2022) 111717, https://doi.org/10.1016/j.foodres.2022.111717.

[36] L. Liu, J. Li, M. Tu, et al., Complete genome sequence provides information on quorum sensing related spoilage and virulence of *Aeromonas salmonicida* GMT3 isolated from spoiled sturgeon, Food Res. Int. 196 (2024) 115039, https://doi.org/10.1016/J.foodres.2024.115039.

[37] X. Han, L. Chen, Z. Hu, et al., Identification of proteins related with pemetrexed resistance by itraq and prm-based comparative proteomic analysis and exploration of IGF2BP2 and FOLR1 functions in non-small cell lung cancer cells, J. Proteomics 237 (2021) 104122, https://doi.org/10.1016/j.jprot.2021.104122.

[38] J. Mi, Z. Yu, H. Yu, et al., Quorum sensing systems in foodborne *salmonella* spp. and corresponding control strategies using quorum sensing inhibitors for food storage, Trends Food Sci. Technol. 144 (2024), https://doi.org/10.1016/J.tifs.2023.104320.

[39] L. Lei, R. Wu, J. Zhang, et al., D-ribose interferes with quorum sensing to inhibit biofilm formation of *Lactobacillus paraplantarum* L-ZS9, Front. Microbiol. 8 (2017) 1860, https://doi.org/10.3389/fmicb.2017.01860.

[40] Y. Zhang, H. Zhong, Y. Gu, et al., Effects of metal ions on signal molecule AI-2 and biofilm of *Lactobacillus fermentation* 733, J. Chin. Inst. Food Sci. Technol. 25 (2025), https://doi.org/10.16429/j.1009-7848.2025.03.006.

[41] L. Liu, R. Wu, J. Zhang, et al., Overexpression of *luxS* promotes stress resistance and biofilm formation of *Lactobacillus paraplantarum* L-ZS9 by regulating the expression of multiple genes, Front. Microbiol. 8 (2018) 2628, https://doi.org/10.3389/fmicb.2018.02628.

[42] Z. Liu, Study on bifidobacterium biofilm formation mechanism and fermentation[D], Jiangnan University, 2022. https://doi.org/10.27169/d.cnki.gwqgu.2022.000102.